separations

MDPI

Article

Single-Step Surface Hydrophilization on Ultrafiltration Membrane with Enhanced Antifouling Property for Pome Wastewater Treatment

Norfadhilatuladha Abdullah [1,2], Norhaniza Yusof [1,2,*], Mohammed Abdullah Dahim [3], Muhammad Faris Hamid [4], Lau Woei Jye [1,2], Juhana Jaafar [1,2], Farhana Aziz [1,2], Wan Norhayati Wan Salleh [1,2], Ahmad Fauzi Ismail [1,2] and Nurasyikin Misdan [5]

1 N29a, Advanced Membrane Technology Research Centre (AMTEC), Universiti Teknologi Malaysia, Johor Bahru 81310, Malaysia
2 Faculty of Chemical and Energy Engineering, Universiti Teknologi Malaysia, Johor Bahru 81310, Malaysia
3 Department of Civil Engineering, King Khalid University, Abha 61421, Saudi Arabia
4 School of Mechanical Engineering, Korea University of Technology and Education, Cheonan 31253, Chungnam, Republic of Korea
5 Faculty of Engineering Technology, Universiti Tun Hussein Onn Malaysia (UTHM), Batu Pahat 86400, Malaysia
* Correspondence: norhaniza@petroleum.utm.my

Abstract: High organic materials in palm oil mill effluent (POME) can result in serious water pollution. To date, biological treatment has been used to reduce the environmental risks of these effluents prior of their discharge into water streams. However, the effluents' dark brownish colour remains as a significant issue that must be addressed, as it affects the overall quality of water. Although membrane technology has been frequently used to address these difficulties, membrane fouling has become a serious limitation in POME treatment. On the other hand, zwitterions with balanced charge groups have received growing interest in the fabrication of antifouling membranes due to their hydrated nature. The development of a simple and efficient covalent bonding technique to improve the stability of zwitterions on membrane surfaces remains a challenge. By grafting and co-depositing polyethylenimine (PEI)-based zwitterion (Z-PEI) with super hydrophilic polydopamine (PDA) on the surface of a commercial polysulfone (PSf) ultrafiltration membrane at ambient temperature, a new zwitterionic surface with a neutral surface charge was created (PDA/Z-PEI). This study aims to investigate the effect of different loading ratios of PDA/Z-PEI (1:1, 1:2, and 1:3) and evaluate their performance on treating brownish coloured anaerobically treated POME (AT-POME). SEM and FTIR analysis showed the successful incorporation of the PDA/Z-PEI membrane while the zwitterionic feature is indicated by zeta potential analysis. Water flux analysis demonstrated that a lower water flux was achieved for M-ZPEI membranes as compared to the PSf and PSf-MDPA membranes, attributed by the tight skin layer of PDA-ZPEI. In the development of a tight hydration layer on the membrane surface by zwitterions, zwitterionic membranes demonstrated excellent antifouling capabilities, particularly PDA/Z-PEI with a loading ratio of (1:2) with a flux recovery ratio of around 84% and colour rejection of 81.75%. Overall, this research contributes to the development of a unique coating with improved stability and antifouling properties by altering the membrane surface in a simple and reliable manner.

Keywords: palm oil mill effluent (POME); ultrafiltration; zwitterion; membrane fouling; polyethylenimine (PEI)

check for updates

Citation: Abdullah, N.; Yusof, N.; Dahim, M.A.; Hamid, M.F.; Jye, L.W.; Jaafar, J.; Aziz, F.; Wan Salleh, W.N.; Ismail, A.F.; Misdan, N. Single-Step Surface Hydrophilization on Ultrafiltration Membrane with Enhanced Antifouling Property for Pome Wastewater Treatment. *Separations* **2023**, *10*, 188. https://doi.org/10.3390/separations10030188

Academic Editor: Mingheng Li

Received: 19 January 2023
Revised: 14 February 2023
Accepted: 27 February 2023
Published: 9 March 2023

Copyright: © 2023 by the authors. Licensee MDPI, Basel, Switzerland. This article is an open access article distributed under the terms and conditions of the Creative Commons Attribution (CC BY) license (https://creativecommons.org/licenses/by/4.0/).

1. Introduction

During the production of palm oil, 50% of the water consumed during the processing of fresh fruit bunches will end up as palm oil mill effluent (POME) [1]. POME contains 95–96% of water, 0.6–0.7% oil, about 4–5% total solid compound and high organic content in which improper disposal of these effluents results in severe pollution to water sources

due to oxygen depletion [2]. For POME treatment, conventional methods mainly focused on the reduction of chemical oxidation demand (COD) and biological oxidative demand (BOD) of the effluent. Nevertheless, treated POME still displays the insignificant removal of colour, which results from the degraded lignin of fruit brunches. Hence, proper treatment is required to ensure that the brownish colour can be filtered and treated.

In general, as compared to other conventional techniques, membrane technology has been widely used for the treatment of wastewater and it has showed an excellent performance in terms of colour removal [3]. However, due to the very high organic content and oil effluent of POME, membranes are prone to bio-fouling and organic fouling caused by non-specific interaction between foulants and membrane surfaces [4–6]. Briefly, fouling is a result of complex physical and chemical interactions between constituents, which are present in feed water with membrane surface [7]. In addition, for post-treating palm mill oil effluent, the impact of fouling may be aggravated due the content of degraded lignin, which is mostly composed of humic acid, a type of organic foulant [8]. Due to that, novel strategies for controlling the impact of fouling on membrane surfaces are required. Over time, fouling seriously affects permeation and rejection, and substantially increases operational and maintenance costs.

To alleviate membrane fouling, the common strategy is to introduce hydrophilic polymers such as poly(ethylene glycol) [9,10], oligosaccharide moieties [11,12], and zwitterionic peptides or polymers [13,14] via blending, surface initiating and grafting, layer-by-layer (LbL), self-assembly and sol gel. Previously, polyethylene glycol (PEG) has been broadly employed in the membrane for elevating the antifouling properties; however, it has been demonstrated that PEG is susceptible to oxidative damage in the presence of oxygen [15]. In recent years, many strategies have been developed to fabricate the membrane with zwitterions. Zwitterionic polymers have attracted a wide interest due to their unique properties of containing both cationic and anionic groups while maintaining electroneutrality and high hydrophilicity [16,17]. As zwitterions are mainly composed of amino acids, the polar solubility of these compound does not have good compatibility with organic solvents, thus blending zwitterions into a polymer matrix seems unpractical [15]. Other strategies include grafting, chemical activation and atomic radical polymerization [15]. Nevertheless, these multi-step strategies are tedious and time consuming. The co-deposition of zwitterions with a self-polymerized material such as dopamine may provide a good anchor of between zwitterions and membrane surface via covalent bond anchoring [17]. The monomer which will be polymerized to polydopamine (PDA) has the unique feature to adhere onto almost all types of surfaces including membrane surfaces, metals and ceramics, attributed to the catechol moieties in its monomeric building blocks [18].

The surface modification of a UF porous membrane by depositing zwitterions is a promising approach to enhance fouling resistibility. The non-fouling behaviour of zwitterions is attributed to their special chemical structure, which bears an equimolar number of anions and cations, to form a tight hydration layer by electrostatic interaction to inhibit the contact between the foulants and membrane surfaces [14,19,20]. To date, numerous studies have been using multi-step preparation for incorporating zwitterions on polymeric membrane. Therefore, herein we attempt to introduce zwitterion via single step co-deposition with self-polymerize dopamine on a UF porous membrane for enhanced fouling-resistant properties. Thus, the influence of the loading ratio and co-deposition time will be thoroughly elucidated, in addition to the overall performance of this developed membrane for colour removal.

2. Methodology

2.1. Materials

Commercial Polysulfone UF membrane ($[C_6H_4\text{-}4\text{-}C(CH_3)_2C_6H_4\text{-}4\text{-}OC_6H_4\text{-}4\text{-}SO_2C_6H_4\text{-}4\text{-}O]_n$ 20 kDa MWCO). Polyethyleneimine (linear PEI, $(C_2H_5N)_n$,M_w 60,000, 50%, Acros Organics, Geel, Belgium),1,3-propanesultone (98%, Sigma-Aldrich, St. Louis, MO, USA), Dimethyl sulfoxide (DMSO, 99.9%, Fisher Scientific, Portsmouth, NH, USA) and acetone

were purchased from HmbG Chemicals. Cellulose acetate dialysis tube 32 kDa was purchased from Sigma-Aldrich. Phosphate buffer solution (PBS, pH 8 ± 0.2, Ultra-Pure Grade) was purchased from Vivantis Technologies, Selangor, Malaysia. Dopamine (DA, $C_8H_{11}NO_2$, 99%) was purchased from Sigma-Aldrich. Real anaerobically treated POME (AT-POME) wastewater was collected at the final discharge area from FGV Palm Industries Berhad, Kulai, Johor, Malaysia. The collected AT-POME was then filtered using vacuum pump before the experiment. Properties of collected AT-POME are presented in Table 1.

Table 1. Characteristics of AT-POME collected at final discharge.

Parameter	Unit	Value
pH	-	8.20
BOD	mg/L	23
COD	mg/L	19
Suspended Solid (SS)	mg/L	101
Oil & Grease (O&G)	mg/L	29
Total Nitrogen (TN)	mg/L	20
Ammonia Nitrogen (AN)	mg/L	0

2.2. Preparation and Characterization of Zwitterionic Polyethyleneimine (Z-PEI)

Overall, 5.0 g of PEI and 15.5 g of 1,3-propanesultone were weighed and separately dissolved in 250 mL and 50 mL DMSO, respectively. The reaction started when the 1,3-propanesultone solution was added in dropwise manner into the stirring PEI solution. The suspension was left stirred and heated at 40 °C for 12 h and then precipitated with 500 mL of acetone. The whole product was dialysed subsequently with distilled water for at least 3 days. The water bath was changed daily to ensure the complete exchange of water and solvent. Lastly, the dialysed product was dehydrated on the hot plate at 60 °C until brown concentrated gel was obtained. The concentrate was finally poured into the Petri dishes and stored in a 60 °C overnight. The final brownish product that was collected was the zwitterionic PEI (Z-PEI).

2.3. Preparation of Zwitterionic Membrane via Co-Deposition Method

Prior to the zwitterionic membrane preparation, the commercial UF membrane was cut (14 cm × 14 cm) and soaked in DI water overnight. For the preparation of the zwitterionic membrane, a solution of Z-PEI with dopamine (DA) was prepared in a phosphate buffer solution (PBS) with each having a concentration of 2 mg/mL, respectively. Next, the soaked membrane was placed on the glass plate and rubber-rolled to remove all the water on the top surface of the membrane. The membrane was later clamped with frames. Subsequently, the prepared Z-PEI solution was poured on the clamped membrane and was left for the co-deposition for 12 h. The remaining solution was removed and the membrane was rinsed with DI water for at least three times followed by being ambient-dried for 30 min and lastly stored in DI water for further use. The produced membrane was labelled as n-ZPEI, where n stands for 1.0, 2.0 and 3.0 ratio of DA to Z-PEI. Meanwhile, PSf and MPDA are the controls used in this study. Table 2 describes the loading concentration used in this study.

Table 2. DA and Z-PEI loading concentrations with their respective membrane annotations.

Membrane Annotation	DA, mg/mL	Z-PEI, mg/mL	Ratio DA: Z-PEI
MPDA	2	0	Control *
1.0-ZPEI	2	2	1:1
2.0-ZPEI	2	4	1:2
3.0-ZPEI	2	6	1:3

* act as the control membrane.

2.4. Characterization of the Zwitterionic Membranes

2.4.1. Physicochemical Properties

Each membrane was characterized based on its physicochemical properties. The characterization methods were scanning electron microscopy (SEM), Fourier transform

infrared (FTIR) spectroscopy, zeta potential and water contact angle goniometry and atomic force microscopic.

Zeta Potential

Dynamic surface charge of each of the produced membranes was determined using a Electrokinetic Zeta potential analyser (Model: Anton Paar SurPASS) equipped with a tuneable gap cell. First, two membrane pieces were cut and attached on the surface of sample holders. The sample holders were then carefully place in the sample housing in a manner of the membrane active surface facing each other. Zeta potential measurements were conducted by using 0.001 M potassium chloride (KCl) solution as dispersant. In the pre-measurement setting of the zeta potential software, the gap height was set at 0.1 mm and the pH was manually adjusted to pH 10 using 0.05 M sodium hydroxide solution (NaOH). During the measurement process, the pH was automatically adjusted to pH 3 by the instrument using 0.05 M hydrochloric acid (HCl).

Scanning Electron Microscopy (SEM)

The top surface and cross sectional morphologies of the membranes were examined by using SEM (Model: Hitachi TM3000, Tokyo, Japan). To examine the surface morphology, a small area of 0.5 cm × 0.5 cm of each membrane cut and observed. For cross-sectional morphologies, membrane samples were dipped in liquid nitrogen and snapped to obtain clean cross-section areas [16]. The examination under SEM was carried out with different magnifications.

Attenuated Total Reflectance-Fourier Transform Infrared (ATR-FTIR)

The surface chemistry of all the membrane including the neat PSf commercial membrane were distinctively analysed using an ATR-FTIR spectrometer (Nicolet iS10, Thermo Scientific, Waltham, MA, USA). Each sample was scanned at wavenumber 500 cm^{-1} to 4000 cm^{-1} and the IR spectra were collected by OMNIC software [21].

Water Contact Angle (WCA)

Hydrophilicity of the produced membranes can be determined by WCA. Contact Angle Goniometer (OCA 15 Pro, Dataphysics, Filderstadt, Germany) via sessile-drop method was used to measure the WCA of each membrane. By using automated driven syringe, 0.50 µL water was drop on the top surface of membrane sample via drop-wise technique. At least 5 values of the contact angles from a random position on the membrane were taken for consistent accuracy.

Membrane Surface Roughness

Atomic force microscope (SPA-300HV, Seiko, Marsiling Ln, Singapore) was used to characterize the surface morphologies of membranes. For this analysis, observation was carried out by scanning the image of samples with an area of 5 µm × 5 µm through non-contact tapping mode.

2.5. Performance Evaluation of the Zwitterionic Membrane

2.5.1. Water Flux

Each membrane was cut to an effective area of 14.6 cm^2. The membrane piece was then inserted into a pressure vessel of the dead-end ultrafiltration system as shown in Figure 1. The membrane was firstly compressed at 3 bar for 30 min. The experiment started with 15 min stabilization at the operating pressure and then the pressure was changed to 2 bar. During the permeation process, the time taken for the permeate to be collected was recorded. Pure water flux is calculated based on the formula Equation (1). Triplicate readings were obtained from 3 coupons of the same membrane.

$$J = \frac{Q}{A\Delta t} \quad (1)$$

where J is water flux (L/m^{2}h), Q is the volume of permeate (L), A is the effective area of the membrane (m^2) and t is the permeate time (h).

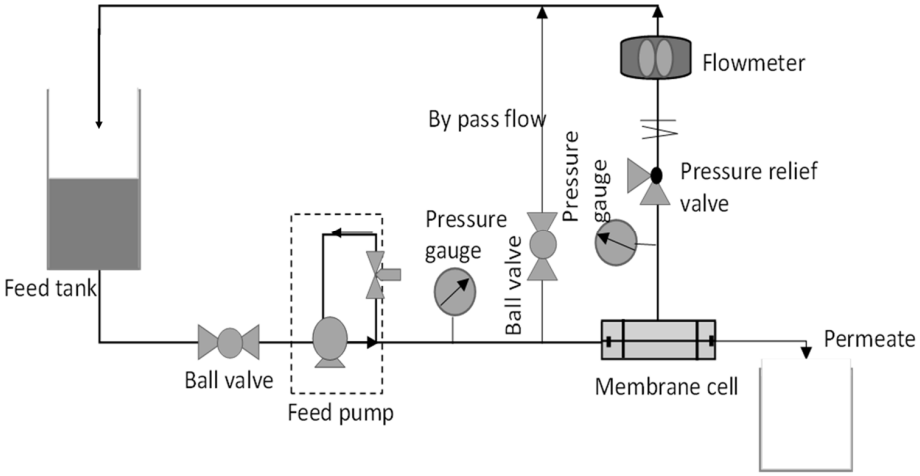


Figure 1. A complete set up of cross flow filtration membrane system.

2.5.2. Rejection of Real Colored POME Wastewater

Real POME wastewater was obtained from the nearby Palm Oil Mill FGV in Kulai, Johor, Malaysia. The collected wastewater was from the final discharge pond right before the release to the water body. The wastewater was non-oily, but highly brownish in colour due to the presence of organic and inorganic matter. Similarly, the steps of the previous experiment were repeated by replacing the feed water with real POME wastewater. Water flux was assessed via Equation (1) and the rejection performance was determined by measuring the reduction total organic carbon (TOC) content in the permeate relative to the feed. Thus, the initial TOC concentration (ppm) in the feed and the final TOC concentration (ppm) in the permeate were analysed by using TOC analyser (Shimadzu, Kyoto, Japan) and the percent rejection was computed by Equation (1).

2.6. Antifouling Performances

The antifouling test was performed by using cross flow filtration membrane system as shown in Figure 1 to simulate the actual membrane processes to reduce fouling propensity. When a flow is applied tangentially across the membrane surface, it is called cross flow filtration. Filtrate passes through the membrane surface when feed flows across it, while the concentrate collects at the opposite end. The membrane's tangential flow causes a shearing effect on the membrane's surface, which lowers fouling [21]. For testing, membrane samples were firstly cut into an effective area of 15.21 cm^2. The membrane was then placed properly into the membrane cell module and DI water was used to fill the feed tank.

Similar to the previous testing, the membrane sample was firstly compressed at 3 bar. Then, the feed was replaced with real POME and operated at 2 bar starting with 15 min stabilization. The antifouling test was carried out for 4 cycles, with 4 h per cycle. For every 20 min, the permeate was collected and water flux was computed. For the POME rejection assessment, the permeate volume was recorded for the first 20 min and the end of the 4th hour for every cycle. The samples were analysed by TOC analyser and the rejection percentages were evaluated. After each 4 h cycle, the membrane was taken out and then went through washing by overnight immersion in DI water. On the next day, the membrane was agitated in the same water for 15 min before starting the next cycle. The cycles continued until achieving 16 h completion. All these steps were then repeated using M-ZPEI 1.0, M-ZPEI 2.0 and M-ZPEI 3.0 membranes.

3. Results and Discussion

3.1. Membrane Characterization

3.1.1. Surface Morphology

The SEM micrograph analysis was used to evaluate the structural morphologies of the control membranes (PSf and PSf-PDA) and PDA/Z-PEI with varied loading ratios (1:1, 1:2 and 1:3). As shown in Figure 2, PSf showed a common morphologies of membrane with finger-like and sponge-like structures. After being coated with PDA, formation of aggregates was observed on the membrane surface. This observation is similar to the studies reported by Xie et al. [17] and Chen et al. [19]. Upon incorporation of Z-PEI, tiny micro gaps are still visible, however, the aggregations decreased when the concentration of PEI increased. In this case, the surface of PDA/Z-PEI with various loading ratios (1:1, 1:2 and 1:3) was significantly smoother and no recognisable aggregates were formed. Such phenomenon can be explained due to non-covalent bonding between PDA molecules, such as π-π stacking and hydrogen bonds, causing the PSf-PDA membrane to aggregate and deposit on top of the membrane surface, whereas covalent cross linking between Z-PEI and PDA via Schiff-base reaction and Michael-addition weakened those weak interactions on the PDA/Z-PEI membrane (π-π stacking and hydrogen bonds) and eventually reduced the appearance of aggregates [20].

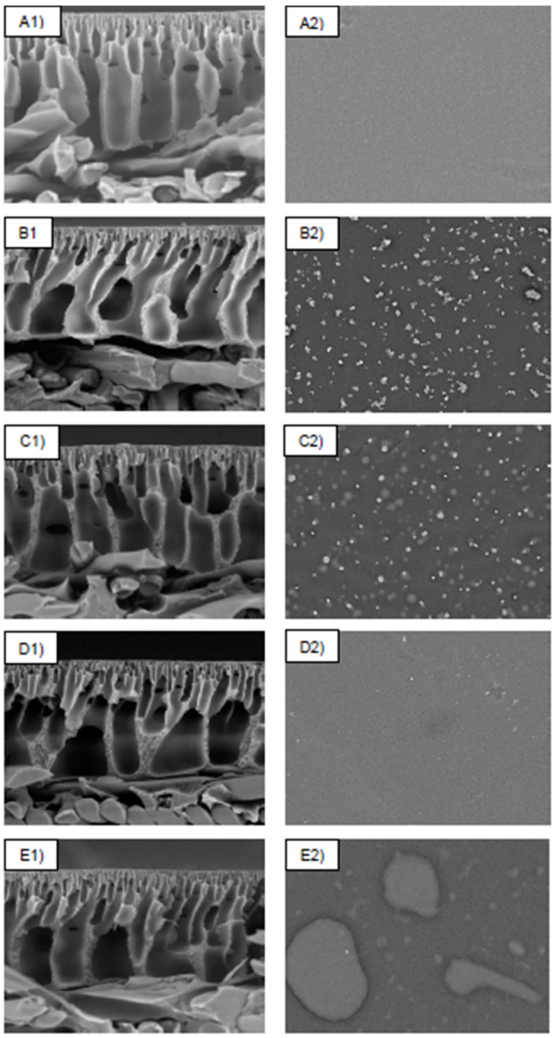


Figure 2. Surface and cross-sectional morphologies of (**A**) PSf, (**B**) PSf-PDA, (**C**) M-ZPEI 1.0, (**D**) M-ZPEI 2.0, and (**E**) M-ZPEI 3.0 with magnification of 1 k (cross-sectional, 50 μm scale) and 1.2 k (surface, 100 μm scale).

These aggregates appeared to have a negative impact on the membrane surface roughness, indicating that the surface morphologies of the PDA/Z-PEI membrane were considerably different from those of the PSf-PDA membrane. As the loading of PDA/Z-PEI increased, the finger-like structures were progressively extended and connected to the porous layer in cross-sectional scans of Figure 2(C1,D1,E1). Figure 2(A1,B1) indicate the development of macro-voids; however, macro-voids are less visible in the membrane where Z-PEI was injected (C1 to E1). This might be due to the inclusion of PDA/Z-PEI, which raises the viscosity of the dope solution. As a result, macro-void formation was decreased [20].

3.1.2. Surface Functional Group

As shown in Figure 3, FTIR was utilised to characterise the presence of functional groups on membrane surfaces. Except for PSf-PDA, the spectra of all PDA/ZPEI membranes displayed a distinct absorption peak at 1039 cm^{-1}, which is attributed to the existence of the SO_3 groups of zwitterionic structure [20]. In comparison, the PSf-PDA spectra does not show this peak, indicating that PDA does not contain any zwitterionic features. On the other hand, the peaks at 1570 and 1650 cm^{-1} refer to the N−H and C−N vibrations of PDA/PEI, indicating that the membrane has been successfully coated with PDA/Z-PEI. Similarly, the absorption peak at 832 cm^{-1} (C–Cl stretching vibration) is more intense in the PSf-PDA membrane, but when Z-PEI loading rises, the depth of the spectrum diminished [22]. These results demonstrated that the quaternary amination process has successfully occurred [15].

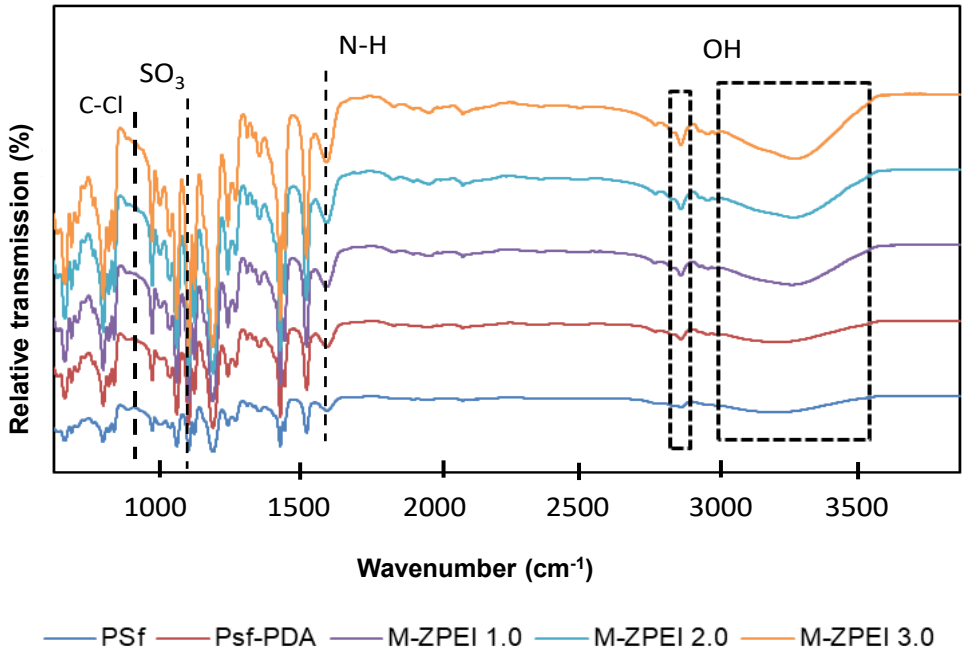


Figure 3. Surface functional group analysis by FTIR of prepared membranes.

3.1.3. Surface Charge

The effect of zwitterionic polymer (Z-PEI) on the surface charge of membranes was characterized by using zeta potential analysis as shown in Figure 4. Based on this figure, at a pH below 5 and 6, all ZPEI membranes are have positive charges. At a pH around 5.0, PSf-PDA membrane and M-ZPEI 1.0 showed iso-electric point (IEP) of 0 mV. The potential values started to turn negative at pH 7.0 (neutral pH), −5 mV for 1.0 Z-PEI, −9 mV for 2.0 Z-PEI, and −22 mV for 3.0 Z-PEI. The zeta potential of the membrane becomes more negative as the loading ratio of Z-PEI increases. This finding indicates that the Z-PEI was hydrated when it was mixed with PDA in a PBS solution [23]. The negatively charged hydrated Z-PEI in the membrane does not dissociate in water [20] due to hydroxide ion

adsorption from water self-ionization [24]. The surface charge should be able to repel the charged solute in the AT-POME to increase colour pigment rejection. As the membrane surface charge became more negative, the colour pigment rejection increased [23].

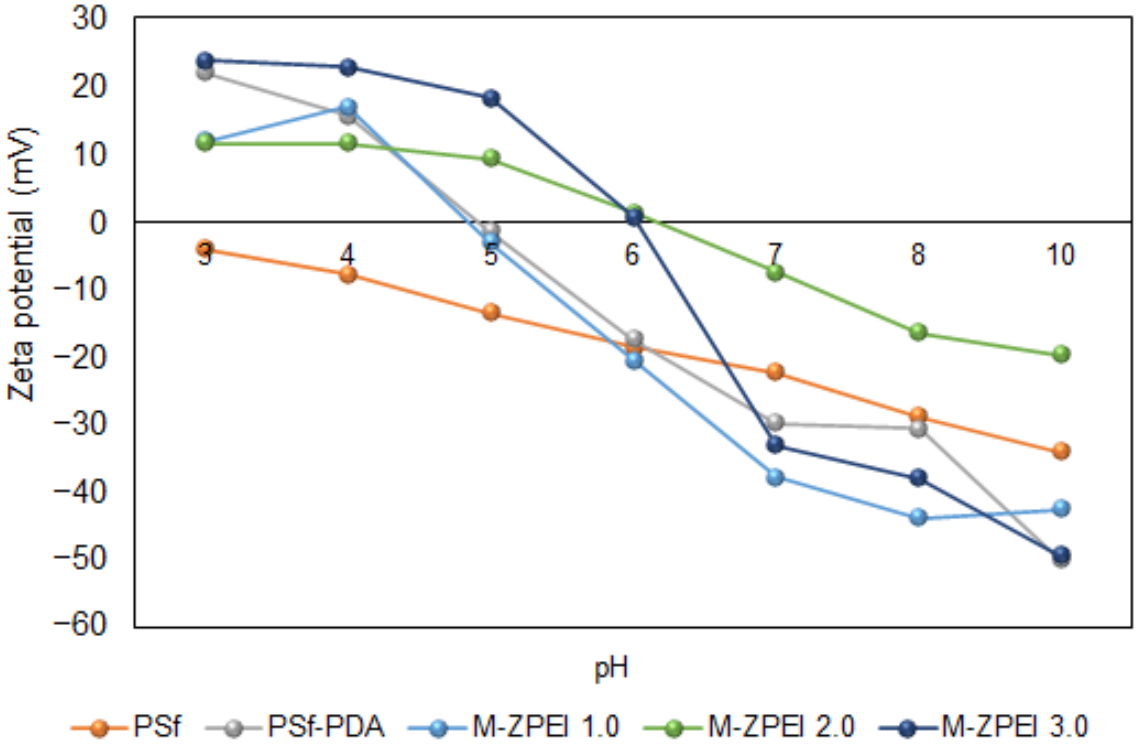
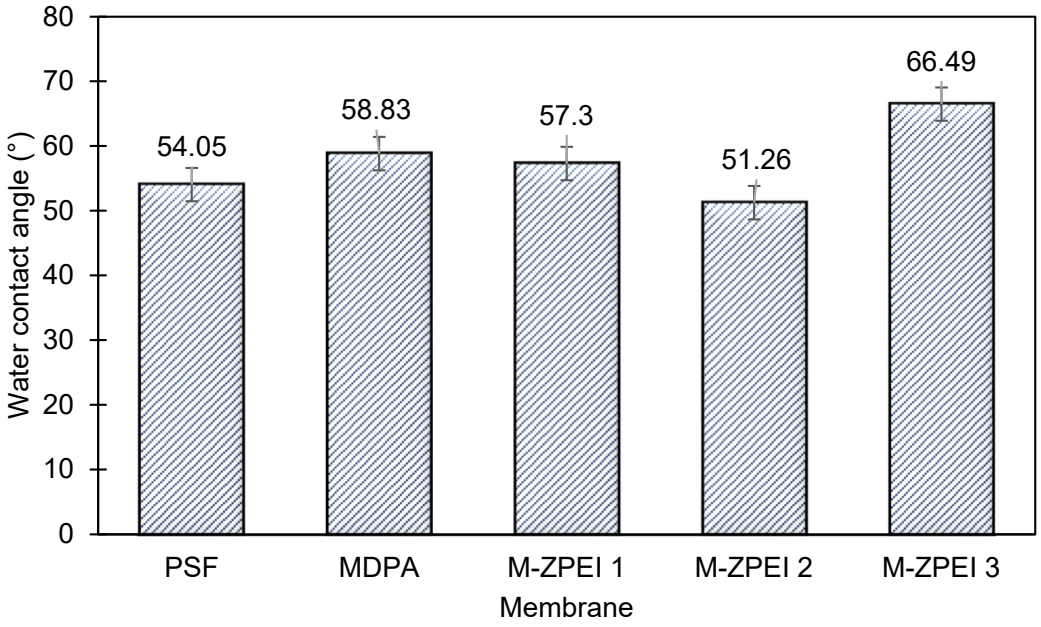


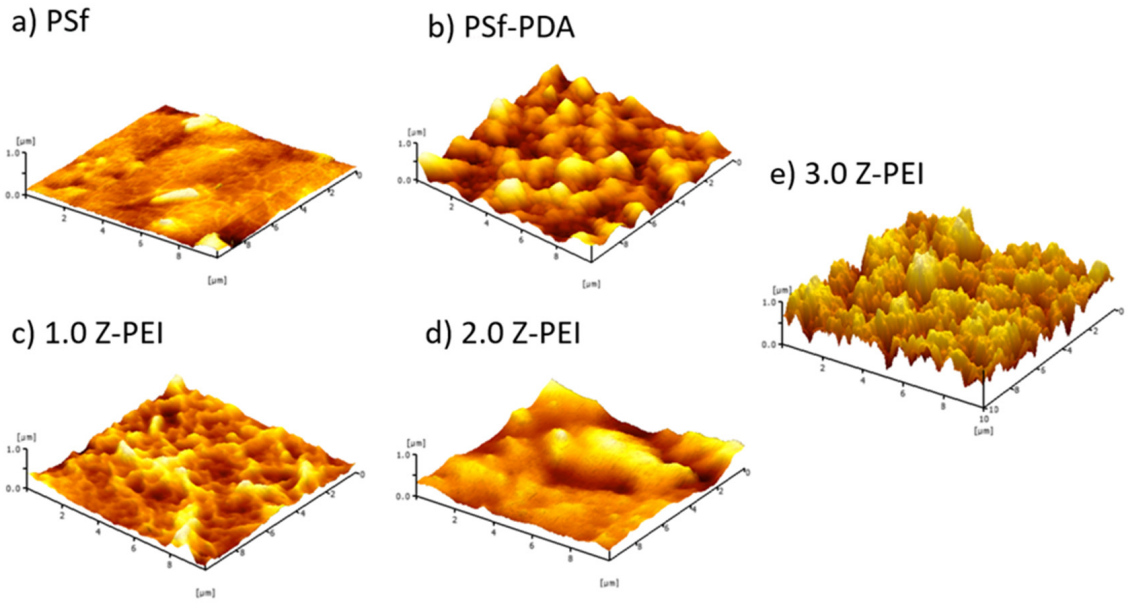
Figure 4. Surface charge of prepared membranes.

3.1.4. Membrane Hydrophilicity

Surface hydrophilicity analysed by the water contact angle (WCA) measurement serves as a good indicator to define the movement of water across the membrane. The composition of membranes and its corresponding surface chemistry has eminent effects, especially in terms of the water interaction which is related to its wettability. In brief, for membranes used for water/wastewater treatment, the hydrophilic surface is often favourable. Membranes with hydrophilic surface typically contain water-loving active functional groups that are able to form "hydrogen-bonds" with water molecules [15]. Based on Figure 5a below, the WCA of the PSf membrane was 54.05°. When PDA was incorporated on the PSf membrane, the WCA increased to 58.83°. Although PDA consists of many amine functional groups that can attract water molecules, their ability is possibly hindered by the stacked aggregates, which caused resistance for water molecules being transported via membrane pores. The stacked aggregates can be further confirmed by AFM images, as shown in Figure 5b. Based on Figure 5b, it can be seen that coating with PDA led to a rougher membrane surface. After that, when Z-PEI was introduced, a slightly lower water contact angle was achieved, due to the interaction of amine groups from PEI and PDA that attracts water molecules to the surface of the membrane.



(**a**)



(**b**)

Figure 5. (**a**) Surface hydrophilicity of prepared membranes; and (**b**) membrane surface roughness images as indicated by AFM.

3.2. Membrane Performance

3.2.1. Water Flux

In brief, pure water permeability (PWP) is defined as the volume of water that passes via membrane per unit time per bar [25]. Briefly, it shows the ability of membranes to generate permeates at a given time. Figure 6 shows the PWP of PSf, PSf-PDA and MZPEI membranes fabricated in this study. From the figure, it can be seen that the water flux of M-ZPEI membranes are lower, ranging from 19.47, 16.44 and 6.1 L/m^2·h for M-ZPEI 1.0,

M-ZPEI 2.0 and M-ZPEI 3.0 as compared to PSf (25.2 L/m^2·h) and PSf-PDA (22.5 L/m^2·h) Initially, it is hypothesized that the water flux will be improved due to the presence of hydrophilic functional groups on PDA and PEI, which attract more water molecules to form a water layer on the surface membrane. However, in this study, we achieved lower water flux for M-ZPEI. We suspected that such aggregates, which initially formed during PDA coating as shown in our previous data, cause an increase in terms of water resistivity. In addition, as the loading of PEI increased, the membrane will have a thicker coating that resulted in water transport resistance, and eventually resulted in a lower water flux. Nevertheless, the thickness of PDA-PEI may assist in a better rejection of colour from AT-POME.

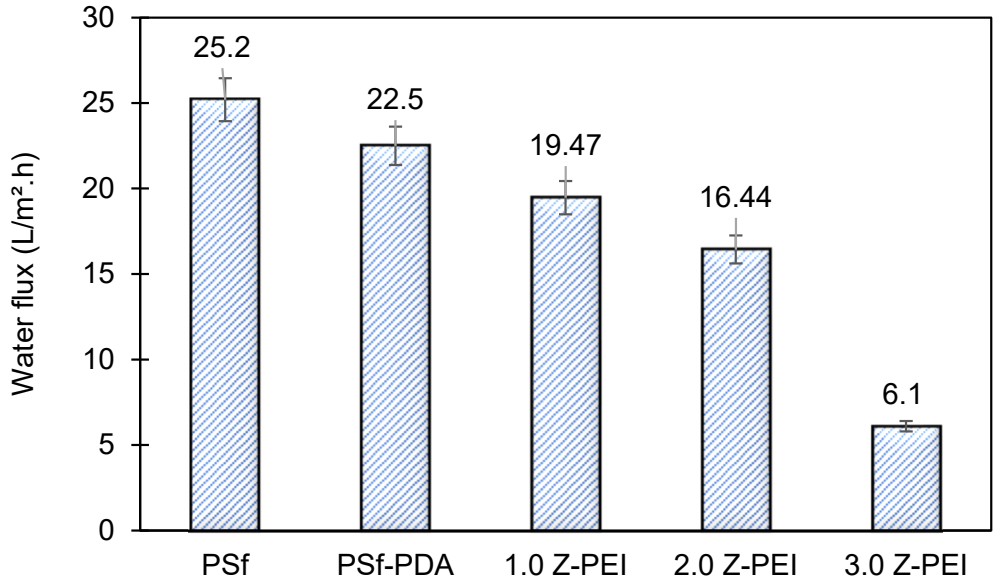


Figure 6. Water flux of all prepared membranes.

3.2.2. Flux Stability and Antifouling Performance

The antifouling property of the membranes was investigated in which the flux of the membranes and their flux recovery ratio (FRR) were evaluated using AT-POME in a cross-flow filtration membrane system. Previous research has shown that water molecules may rearrange and firmly attach on zwitterionic groups via electrostatic interaction, forming a hydration layer that can prevent foulant contact with the membrane surface [26,27]. As a result, the accumulated foulants may be eliminated using water washing, thereby preventing irreversible fouling as shown in Figure 7. Figure 8a shows results of antifouling evaluation after four cycles by PSf, PSf-PDA, and Z-PEI membranes. Even though the initial fluxes of controlled membranes (25.2 L/m^2·h for PSf and 22.5 L/m^2·h for PSf-PDA) were higher than modified PDA/Z-PEI membranes (19.47 L/m^2·h, 16.44 L/m^2·h for ZPEI 1.0, ZPEI2.0 PDA/Z-PEI and 5.92 L/m^2·h for 3.0 PDA/Z-PEI), but the control membranes experienced severe fouling, hence the flux drop was very significant in every cycle. On the other hand, ZPEI membranes have shown excellent antifouling property by managing the better stability of the membranes. This is attributed to the covalent connection established between the Z-PEI and PDA membranes, which then provide a stable antifouling feature to the PDA/Z-PEI membrane [20].

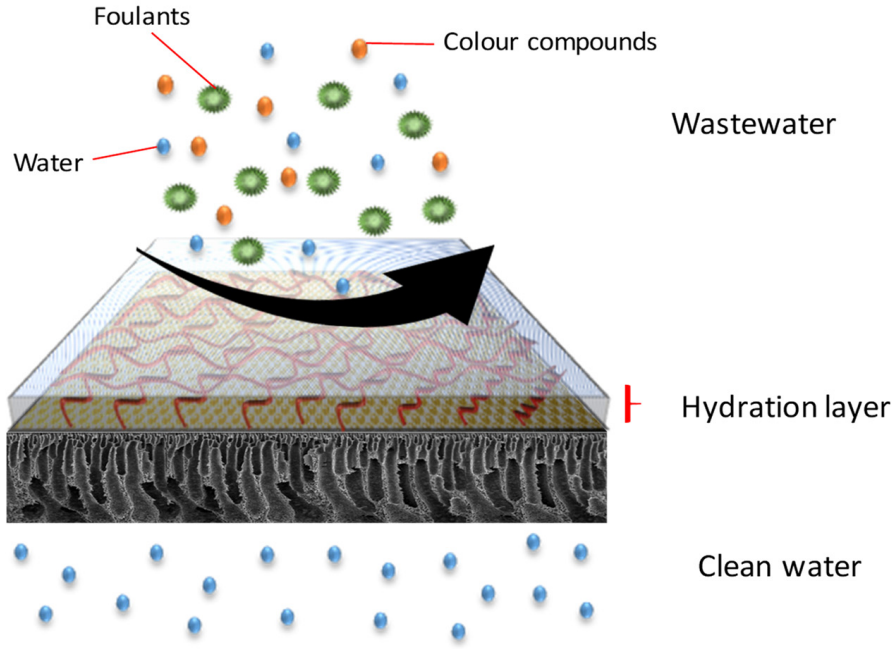
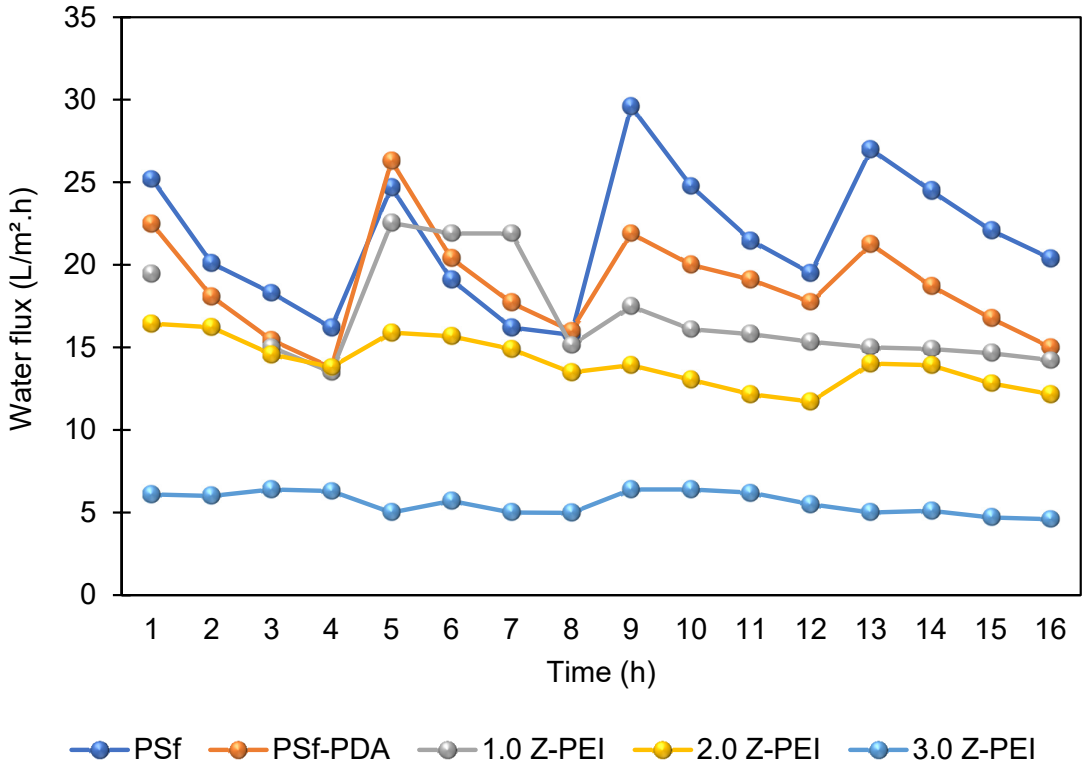
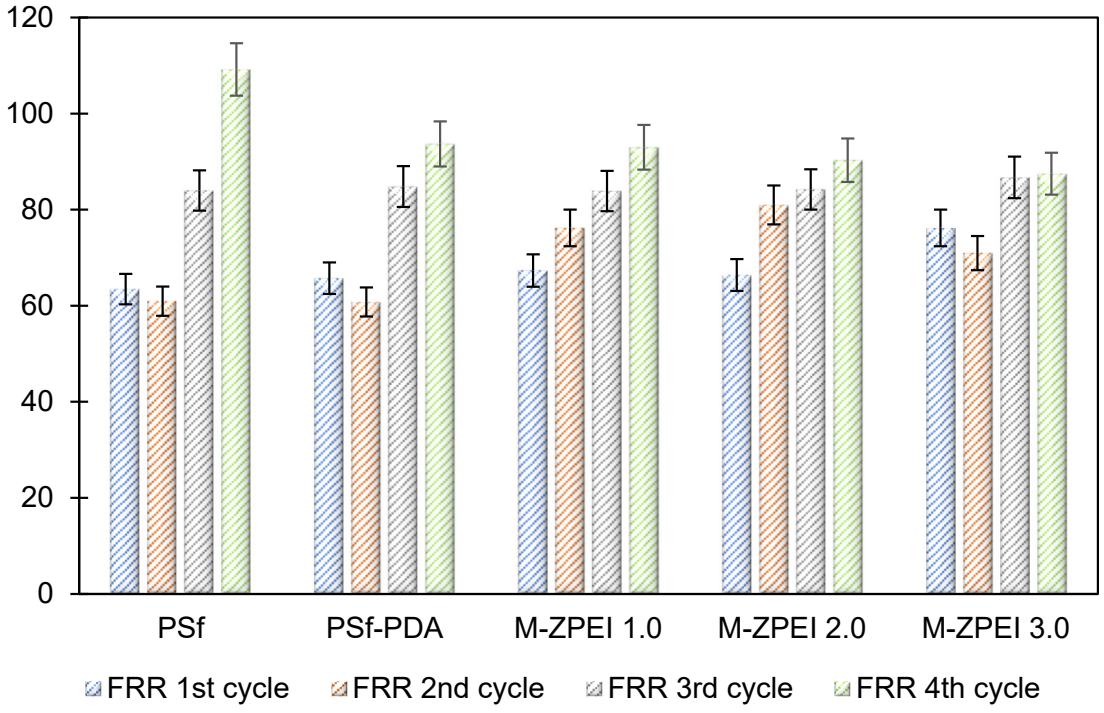


Figure 7. Antifouling behaviour of DA/Z-PEI.



(**a**)

Figure 8. *Cont.*



(**b**)

Figure 8. (**a**) Water flux profile of prepared membranes at in four filtration cycles; and (**b**) FRR values of all prepared membrane after four cycles.

Based on FRR %, ZPEI membranes exhibited higher FRR than the controlled membranes. The FRR in values for four cycles for PSf membrane and PSf-PDA membrane is between 60.8% to 81%, showing poor antifouling property. Meanwhile, the FRR values for M-ZPEI 2.0 and M-ZPEI 3.0 for four cycles of operation (84% above), proving better antifouling performances for both membranes. From this result, it is clear that M-ZPEI 2.0 and M-Z-PEI 3.0 have superior stability and antifouling properties after a long filtration duration. Among M-ZPEI 2.0 and M-ZPEI 3.0, it is advantageous to choose M-ZPEI 2.0 over M-ZPEI 3.0 due to the optimal performance of M-ZPEI 2.0 in maintaining membrane integrity in both flux and FRR. Based on this, it can be concluded that one of the best ways to combat fouling on membrane surfaces is to use a membrane with a negatively charged surface that repels and prevents foulant deposition. Fouling of the membrane can be reduced in this way.

3.2.3. Rejection of Real POME Wastewater

Figure 9 reveals the colour rejection exhibited by the membranes for four cycles of operation. As M-ZPEI 2.0 possesses a more practical flux against AT-POME and also optimal FRR compared with M Z-PEI 3.0, M-ZPEI 2.0 was chosen for the colour removal test. The PSf membrane showed an unstable trend where the colour rejection rises in the 2nd cycle to (78.1%), drops drastically in the 3rd cycle to (37.96%) and then jump back to (74.45%) in the 4th cycle. Based on this finding, the PSf membrane shows the instability of the membrane in holding its integrity on maintaining its colour rejection performance. In addition, such inconsistent colour rejection can also be attributed to fouling, whereby that higher rejection at the last cycle is due to the deposition of foulants from POME water on the membrane surface. It is acknowledged that deposition of foulants will result in better molecules resistance, in scarification of the water flux [28].

On the other hand, for the PSf-PDA membrane, the trend was clearly shown in a descending order, which projects a poor colour rejection ability by the PSf-PDA membrane. Although the membranes were endowed with superhydrophilicity as a result of the hierar-

chical structure created by the PDA nanocluster, their lack of flexibility and stretch ability would severely limit their long-term usage in practical applications [29]. In this case, it is possible that delamination of PDA coating occurs, and eventually results in open pores that allow the movement of colour molecules across the membrane layer. On the other hand, it was evident that M-ZPEI 2.0 showed an excellent colour rejection performance over AT-POME. For the four cycles it has maintained the highest and the most stable colour rejections of 78.10%, 81.75%, 78.10%, and 81.75%. This proves that M-ZPEI 2.0 worked very well in rejecting the colour particles from the AT-POME and also managed to maintain its performance by not declining in colour rejection (%) significantly. In addition, a very stable water flux was obtained when M-ZPEI 2.0 was tested. Therefore, it is proved that the M-ZPEI 2.0 membrane has great potential to be used to tackle severe colour issues coming from POME.

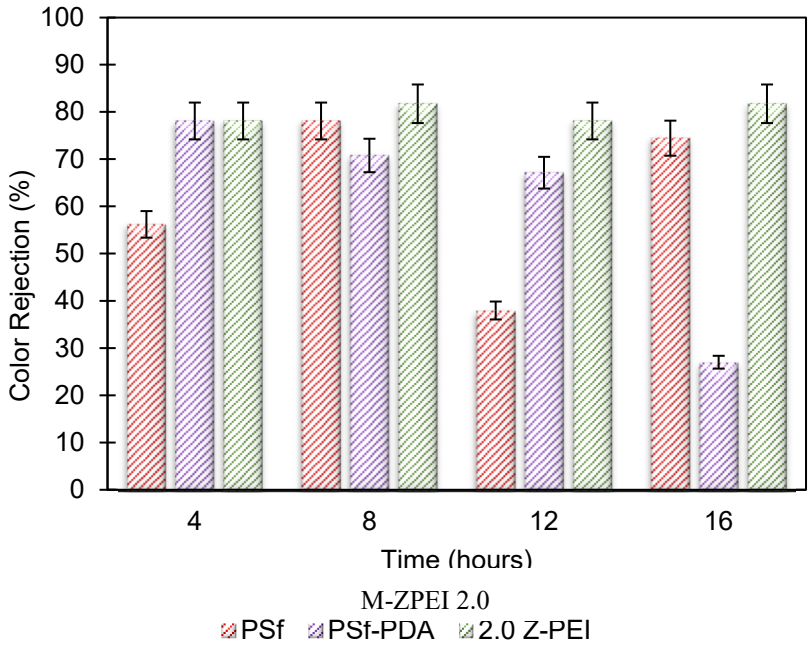


Figure 9. Rejection of coloured POME water by using PSf, PSf-PDA and M-ZPEI 2.0.

4. Conclusions and Future Direction

In this study, we prepared a stable antifouling coating on the material surface via a one-step co-deposition of PDA and zwitterionic polymer (Z-PEI). SEM analysis showed that a membrane with PDA having aggregates and the formation of aggregates was reduced when PEI was incorporated. Z-PEI added to PSf membranes might dramatically increase antifouling performance. FTIR analysis has shown major peaks related to the zwitterionic properties of these materials. The surface charge demonstrated that ZPEI membranes attained their zwitterionic properties at pH 6.0. A stability test demonstrated that this membrane is able to be used and the ZPEI membrane has better water flux stability after four filtration cycles. Colour rejection showed M-ZPEI 2.0 can maintain its performance by not declining in colour rejection.

In this study, the future direction should be linked to a deeper understanding in terms of stability over a longer period of time so that any effect of delamination of zwitterionic PEI can be thoroughly observed. Other aspects such as long-term antifouling effect, performance of water flux and permeation over continuous operating systems should also be studied. As this method is viable due to a simple chemical and synthesis period, all of the above aspects should be thoroughly studied prior to commercialization.

Author Contributions: Conceptualization, N.A. and M.F.H.; methodology, N.A. and M.F.H.; validation, N.A., M.F.H. and L.W.J.; formal analysis, N.A., M.F.H. and L.W.J.; investigation, N.A. and M.F.H.; resources, N.Y., J.J., F.A., W.N.W.S., A.F.I. and N.M.; data curation, N.A.; writing—original draft preparation, N.A., N.Y. and M.F.H.; writing—review and editing, N.A., N.Y., M.A.D., L.W.J., J.J., F.A., W.N.W.S., A.F.I. and N.M.; visualization, N.A. and M.F.H.; supervision, N.Y., L.W.J., J.J., F.A., W.N.W.S., A.F.I. and N.M.; project administration, N.Y., M.A.D., L.W.J., J.J., F.A., W.N.W.S., A.F.I. and N.M.; funding acquisition, N.Y., M.A.D., L.W.J., J.J., F.A., W.N.W.S., A.F.I. and N.M. All authors have read and agreed to the published version of the manuscript.

Funding: This research was funded by the Ministry of Higher Education (MoHE) Malaysia as part of the FRGS grant [FRGS/1/2022/STG05/UTM/02/10] and Universiti Teknologi Malaysia as part of UTM Shine Grant [No. Q.J130000.2451.09G21]. The first author would like to acknowledge the Zamalah scholarship received from Universiti Teknologi Malaysia. The authors also extend their appreciation to the Deanship of Scientific Research, King Khalid University for funding part of this work through General Research Project under grant number GRP-2-95-43.

Data Availability Statement: Data is contained within the article. The data presented in this study are as shown in the article.

Acknowledgments: This research was funded by the Ministry of Higher Education (MoHE) Malaysia as part of the FRGS grant [FRGS/1/2022/STG05/UTM/02/10] and Universiti Teknologi Malaysia as part of UTM Shine Grant [No. Q.J130000.2451.09G21]. The first author would like to acknowledge the Zamalah scholarship received from Universiti Teknologi Malaysia. The authors also extend their appreciation to the Deanship of Scientific Research, King Khalid University for funding part of this work through General Research Project under grant number GRP-2-95-43.

Conflicts of Interest: The authors declare no conflict of interest.

References

1. Mamimin, C.; Singkhala, A.; Kongjan, P.; Suraraksa, B.; Prasertsan, P.; Imai, T.; O-Thong, S. Two-stage thermophilic fermentation and mesophilic methanogen process for biohythane production from palm oil mill effluent. *Int. J. Hydrogen Energy* **2015**, *40*, 6319–6328. [CrossRef]
2. Mahmod, S.S.; Takriff, M.S.; Al-Rajabi, M.M.; Abdul, P.M.; Gunny, A.A.N.; Silvamany, H.; Jahim, J.M. Water reclamation from palm oil mill effluent (POME): Recent technologies, by-product recovery, and challenges. *J. Water Process Eng.* **2023**, *52*, 103488. [CrossRef]
3. Subramaniam, M.N.; Goh, P.S.; Kau, W.J.; Ismail, A.F. At-pomeAT-POME colour removal through photocatalytic submerged filtration using antifouling PVDF-TNT nanocomposite membrane. *Sep. Purif. Technol.* **2018**, *191*, 266–275. [CrossRef]
4. Harby, N.F.A.; El-Batouti, M.; Elewa, M. Prospects of Polymeric Nanocomposite Membranes for Water Purification and Scalability and their Health and Environmental Impacts: A Review. *Nanomaterials* **2022**, *12*, 3637. [CrossRef]
5. Batouti, M.E.; Alharby, N.F.; Elewa, M.M. Review of New Approaches for Fouling Mitigation in Membrane Separation Processes in Water Treatment Application. *Separations* **2021**, *9*, 1. [CrossRef]
6. Ho, K.C.; Teow, Y.H.; Ang, W.L.; Mohammad, A.W. Novel GO/OMWCNTs mixed-matrix membrane with enhanced antifouling property for palm oil mill effluent treatment. *Sep. Purif. Technol.* **2017**, *177*, 337–349. [CrossRef]
7. Choudhury, R.R.; Gohil, J.M.; Mohanty, S.K.; Nayak, S.K. Antifouling, fouling release and antimicrobial materials for surface modification of reverse osmosis and nanofiltration membranes. *J. Mater. Chem. A* **2018**, *6*, 313–333. [CrossRef]
8. Zhu, L.J.; Zhu, L.P.; Zhao, Y.F.; Zhu, B.K.; Xu, Y.Y. Anti-fouling and anti-bacterial polyethersulfone membranes quaternized from the additive of poly(2-dimethylamino ethyl methacrylate) grafted SiO_2 nanoparticles. *J. Mater. Chem. A* **2014**, *2*, 15566–15574. [CrossRef]
9. Etemadi, H.; Yegani, R.; Seyfollahi, M.; Rabiee, M. Synthesis, characterization, and anti-fouling properties of cellulose acetate/polyethylene glycol-grafted nanodiamond nanocomposite membranes for humic acid removal from contaminated water. *Iran. Polym. J.* **2018**, *27*, 381–393. [CrossRef]
10. Mondal, M.; De, I.S. Characterization and antifouling properties of polyethylene glycol doped PAN–CAP blend membrane. *RSC Adv.* **2015**, *5*, 38948–38963. [CrossRef]
11. Nurioglu, A.G.; Esteves, A.C.C.; With, G. With, Non-toxic, non-biocide-release antifouling coatings based on molecular structure design for marine applications. *J. Mater. Chem. B* **2015**, *3*, 6547–6570. [CrossRef]
12. Zen, F.; Angione, M.D.; Behan, J.A.; Cullen, R.J.; Duff, T.; Vasconcelos, J.M.; Scanlan, E.M.; Colavita, P.E. Modulation of Protein Fouling and Interfacial Properties at Carbon Surfaces via Immobilization of Glycans Using Aryldiazonium Chemistry. *Sci. Rep.* **2016**, *6*, 24840. [CrossRef]
13. He, M.; Gao, K.; Zhou, L.; Jiao, Z.; Wu, M.; Cao, J.; You, X.; Cai, Z.; Su, Y.; Jiang, Z. Zwitterionic materials for antifouling membrane surface construction. *Acta Biomater.* **2016**, *40*, 142–152. [CrossRef]

14. Zhao, D.; Qiu, G.; Li, X.; Wan, C.; Lu, K.; Chung, T.-S. Zwitterions coated hollow fiber membranes with enhanced antifouling properties for osmotic power generation from municipal wastewater. *Water Res.* **2016**, *104*, 389–396. [CrossRef]
15. Zhu, J.; Su, Y.; Zhao, X.; Li, Y.; Zhang, R.; Fan, X.; Ma, Y.; Jiang, Z. Constructing a zwitterionic ultra fi ltration membrane surface via multisite anchorage for superior long-term antifouling properties. *RSC Adv.* **2015**, *5*, 40126–40134. [CrossRef]
16. Lau, S.K.; Yong, W.F. Recent Progress of Zwitterionic Materials as Antifouling Membranes for Ultrafiltration, Nanofiltration, and Reverse Osmosis. *Langmuir* **2021**, *3*, 4390–4412. [CrossRef]
17. Xie, Y.; Chen, S.; Zhang, X.; Shi, Z.; Wei, Z.; Bao, J.; Zhao, W.; Zhao, C. Engineering of Tannic Acid Inspired Antifouling and Antibacterial Membranes through Co-deposition of Zwitterionic Polymers and Ag Nanoparticles. *Ind. Eng. Chem. Res.* **2019**, *58*, 11689–11697. [CrossRef]
18. Singh, I.; Dhawan, G.; Gupta, S.; Kumar, P. Recent Advances in a Polydopamine-Mediated Antimicrobial Adhesion System. *Front. Microbiol.* **2021**, *11*, 2020. [CrossRef] [PubMed]
19. Chen, S.; Xie, Y.; Xiao, T.; Zhao, W.; Li, J.; Zhao, C. Tannic acid-inspiration and post-crosslinking of zwitterionic polymer as a universal approach towards antifouling surface. *Chem. Eng. J.* **2018**, *337*, 122–132. [CrossRef]
20. Yao, L.; He, C.; Chen, S.; Zhao, W.; Xie, Y.; Sun, S.; Nie, S.; Zhao, C. Codeposition of Polydopamine and Zwitterionic Polymer on Membrane Surface with Enhanced Stability and Antibiofouling Property. *Langmuir* **2019**, *35*, 1430–1439. [CrossRef]
21. Tajuddin, M.H.; Yusof, N.; Abdullah, N.; Abidin, M.N.Z.; Salleh, W.N.W.; Ismail, A.F. Incorporation of layered double hydroxide nanofillers in polyamide nanofiltration membrane for high performance salt rejections. *J. Taiwan Inst. Chem. Eng.* **2019**, *97*, 1–11. [CrossRef]
22. Gopalakrishnan, K.; Subrahmanyam, K.S.; Kumar, P.; Govindaraj, A.; Rao, C.N.R. Reversible chemical storage of halogens in few-layer graphene. *RSC Adv.* **2012**, *2*, 1605–1608. [CrossRef]
23. Tan, Y.H.; Goh, P.S.; Ismail, A.F.; Ng, B.C.; Lai, G.S. Decolourization of aerobically treated palm oil mill effluent (AT-POME) using polyvinylidene fluoride (PVDF) ultrafiltration membrane incorporated with coupled zinc-iron oxide nanoparticles. *Chem. Eng. J.* **2017**, *308*, 359–369. [CrossRef]
24. Breite, D.; Went, M.; Prager, A.; Schulze, A. Tailoring membrane surface charges: A novel study on electrostatic interactions during membrane fouling. *Polymers* **2015**, *7*, 2017–2030. [CrossRef]
25. Lau, W.J.; Ismail, A.F.; Goh, P.S.; Hilal, N.; Ooi, B.S. Characterization methods of thin film composite nanofiltration membranes. *Sep. Purif. Rev.* **2015**, *44*, 135–156. [CrossRef]
26. Yang, H.C.; Liao, K.J.; Huang, H.; Wu, Q.Y.; Wan, L.S.; Xu, Z.K. Mussel-inspired modification of a polymer membrane for ultra-high water permeability and oil-in-water emulsion separation. *J. Mater. Chem. A* **2014**, *2*, 10225–10230. [CrossRef]
27. Schlenoff, J.B. Zwitteration: Coating surfaces with zwitterionic functionality to reduce nonspecific adsorption. *Langmuir* **2014**, *30*, 9625–9636. [CrossRef]
28. Ju, J.; Wang, C.; Wang, T.; Wang, Q. Preparation and characterization of pH-sensitive and antifouling poly(vinylidene fluoride) microfiltration membranes blended with poly(methyl methacrylate-2-hydroxyethyl methacrylate-acrylic acid). *J. Colloid Interface Sci.* **2014**, *15*, 175–180. [CrossRef]
29. Huang, X.; Zhang, S.; Xiao, W.; Luo, J.; Li, B.; Wang, L.; Xue, H.; Gao, J. Flexible PDA@ACNTs decorated polymer nanofiber composite with superhydrophilicity and underwater superoleophobicity for efficient separation of oil-in-water emulsion. *J. Membr. Sci.* **2020**, *614*, 118500. [CrossRef]

Disclaimer/Publisher's Note: The statements, opinions and data contained in all publications are solely those of the individual author(s) and contributor(s) and not of MDPI and/or the editor(s). MDPI and/or the editor(s) disclaim responsibility for any injury to people or property resulting from any ideas, methods, instructions or products referred to in the content.